

# Using photoemission spectroscopy to probe a strongly interacting Fermi gas

J. T. Stewart, J. P. Gaebler, and D. S. Jin\*

*JILA, Quantum Physics Division, National Institute of Standards and Technology and Department of Physics, University of Colorado, Boulder, CO 80309-0440, USA*

Ultracold atom gases provide model systems in which many-body quantum physics phenomena can be studied. Recent experiments on Fermi gases have realized a phase transition to a Fermi superfluid state with strong interparticle interactions [1, 2, 3, 4, 5, 6, 7]. This system is a realization of the BCS-BEC crossover connecting the physics of BCS superconductivity and that of Bose-Einstein condensation (BEC) [8, 9, 10]. While many aspects of this system have been investigated, it has not yet been possible to measure the single-particle excitation spectrum, which is a fundamental property directly predicted by many-body theories. Here we show that the single-particle spectral function of the strongly interacting Fermi gas at  $T \approx T_c$  is dramatically altered in a way that is consistent with a large pairing gap. We use photoemission spectroscopy to directly probe the elementary excitations and energy dispersion in the Fermi gas of atoms. In these photoemission experiments, an rf photon ejects an atom from our strongly interacting system via a spin-flip transition to a weakly interacting state. We measure the occupied single-particle density of states for an ultracold Fermi gas of  $^{40}\text{K}$  atoms at the cusp of the BCS-BEC crossover and on the BEC side of the crossover, and compare these results to that for a nearly ideal Fermi gas. Our results probe the many-body physics in a way that could be compared to data for high- $T_c$  superconductors [11]. This new measurement technique for ultracold atom gases, like photoemission spectroscopy for electronic materials, directly probes low energy excitations and thus can reveal excitation gaps and/or pseudogaps. Furthermore, this technique can provide an analog to angle-resolved photoemission spectroscopy (ARPES) for probing anisotropic systems, such as atoms in optical lattice potentials.

As interacting quantum systems with highly tunable parameters and well understood two-body interactions, ultracold atom gases provide model systems in which to test condensed matter theories. A challenge for experimenters is to find ways to probe these atom gases that relate directly to condensed matter ideas and enable sensitive searches for new phenomena that can advance our understanding of strongly correlated systems. At a very basic level, the effect of interactions is a modification of

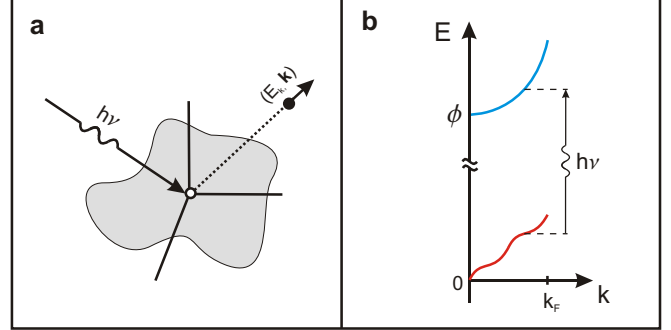


FIG. 1: **Photoemission spectroscopy for ultracold atom gases.** **a** In electron PES, one measures the energy of electrons emitted from solids, liquids, or gases by the photoelectric effect. Using energy conservation, the original energy of the electrons in the substance can be determined. Similarly, in photoemission spectroscopy for atoms, an rf photon with energy,  $h\nu$ , transfers atoms into a weakly interacting spin state. **b** The rf photon drives a vertical transition where the momentum  $\hbar k$  is essentially unchanged. By measuring the energy and momentum of the out-coupled atoms (upper curve) we can determine the quasiparticle excitations and their dispersion relation (lower curve). Here  $\phi$  is the Zeeman energy difference between the two different spin states of the atom.

the single-particle states. As interactions are increased, the single-particle eigenstates of the non-interacting case become quasi-particles and phase transitions manifest themselves as qualitative changes to the excitation spectrum [12], such as the appearance of energy gaps. The single-particle excitation spectrum can be predicted by many-body theory and is a fundamental property of any interacting system.

For electronic systems, photoemission spectroscopy (PES) provides a powerful technique to probe the occupied single-particle states [13]. In a typical PES experiment, electrons are ejected from a substance through the photoelectric effect, see Fig. 1a. The photoelectrons are collected, energy and momentum resolved, and counted to give a spectrum of intensity as a function of the measured kinetic energy,  $\epsilon_k = \hbar^2 k^2 / 2m$ . Here,  $\hbar = h/2\pi$ , where  $h$  is Planck's constant, and  $m$  is the particle mass. By conservation of energy, one can determine the energy of the original single-particle state,  $E_s$ , using

$$E_s = \epsilon_k + \phi - h\nu. \quad (1)$$

Here,  $h\nu$  is the photon energy,  $\phi$  is the work function of the surface, and  $E_F - E_s$  is often referred to as the binding energy [13].

For ultracold atom gases, radio-frequency (rf) spectroscopy has been used to probe a strongly interacting Fermi gas [1, 3, 14, 15, 16, 17, 18]. In a typical experiment, a pulse of rf drives atoms into an unoccupied Zeeman spin state, where they are counted to yield a spectrum of counts versus rf frequency. To date, the rf out-coupled atoms have not been energy or momentum resolved. However, analogous to electron PES, the momentum of the rf photon is negligible compared to the typical momentum of the atoms and therefore the momenta of the out-coupled atoms are characteristic of the original atom states. Eqn. 1 applies to photoemission spectroscopy of atom gases, by means of momentum-resolved rf spectroscopy, if one simply replaces the work function  $\phi$  with the Zeeman energy splitting, see Fig. 1b. The extension of photoemission spectroscopy from condensed matter to cold Fermi gases was discussed by Dao *et al.* [19].

In this paper, we use photoemission spectroscopy, by means of momentum-resolved rf spectroscopy, to probe an ultracold gas of fermionic  $^{40}\text{K}$  atoms. Similar to PES in solids, this measurement probes the single-particle spectral function, which is directly related to the single-particle Green's function predicted by many-body theories [13]. We use this new technique to probe the Fermi gas near a magnetic-field Fano-Feshbach resonance where one can tune strong atom-atom interactions to realize a Fermi superfluid in the region of the BCS-BEC crossover [1, 2, 3, 4, 5, 6, 7].

Our Fermi gas consists of  $3 \times 10^5$   $^{40}\text{K}$  atoms in a mixture of two spin-states. The gas is confined in an optical dipole trap and evaporatively cooled to  $T/T_F = 0.18$ , where  $T$  is the temperature,  $T_F$  is the Fermi temperature as defined by  $T_F = E_F/k_B$ , and  $k_B$  is Boltzmann's constant. The Fermi energy,  $E_F = h \cdot (9.4 \pm 0.5 \text{ kHz})$ , is determined from a measurement of the peak density of the trapped gas. For the photoemission spectroscopy, we apply an rf pulse that couples atoms in one of the two spin states to an unoccupied third spin state. There are two essential requirements for determining the excitation spectrum. The first is that the interaction energy is sufficiently small that  $\epsilon_k = \hbar^2 k^2 / 2m$  holds and the data are not subject to complicated final-state effects [20, 21, 22, 23, 24, 25, 26]. The second requirement is that collisions do not scramble the energy and momentum information carried by the out-coupled atoms. In previous rf spectroscopy measurements both of these requirements were not satisfied [3, 15, 16, 17, 18]. In our  $^{40}\text{K}$  gas, however, the interaction energy for the out-coupled atoms is approximately 640 Hz, which is much smaller than  $E_F$ . Furthermore, the mean-free path for the out-coupled atoms is much larger than the size of the gas:  $\frac{1}{\sigma n} \approx 6 R_F$ , where  $\sigma$  is collision cross section,  $n$  is the average density, and  $R_F$  is the Fermi radius of the non-interacting gas.

To resolve the kinetic energy,  $\epsilon_k$ , of the rf out-coupled

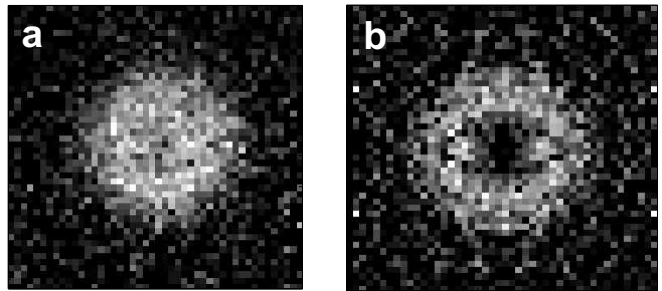


FIG. 2: **Extracting the 3D momentum distribution.** **a** A time-of-flight absorption image ( $\sim 145\mu\text{m} \times 145\mu\text{m}$ ) of atoms that have been transferred into a third spin state is taken after applying an rf pulse to a Fermi gas on the BEC side of the Feshbach resonance. **b** After performing quadrant averaging we use an inverse Abel transform to reconstruct the 3D momentum distribution. For this particular example, a 2D slice at the center reveals a shell-like structure for the momentum distribution of the out-coupled atoms.

atoms we apply an rf pulse that is short compared to the trap period. We then immediately turn off the trap, let the gas ballistically expand, and measure the velocity distribution using state-selective time-of-flight absorption imaging, see Fig. 2. Assuming a symmetric momentum distribution, we extract the 3D momentum distribution of the out-coupled atoms from the 2D image by performing an inverse Abel transform.

We first consider the case of an ideal Fermi gas. To create a very weakly interacting gas we adiabatically ramp the magnetic field to the zero crossing of the Feshbach resonance. In Fig. 3a, we plot the intensity, which is proportional to the number of atoms transferred into the third spin state, as a function of the original single-particle energy  $E_s$  and wave vector  $k$ . The data are obtained by varying the rf frequency and counting the out-coupled atoms as a function of their momenta. We define zero energy to be the energy of a non-interacting atom at rest in the initial spin state. The intensity map for a non-interacting Fermi gas is expected to show delta function peaks at  $E_s = \epsilon_k$ . The white asterisks mark the centers of the intensity at each value of  $k$  as determined from Gaussian fits; these show good agreement with the expected dispersion (black line). The rms width in  $E_s$  of the measured spectrum in Fig. 3a is 2.1 kHz and is due to an energy resolution that comes from the rf pulse duration.

To create a strongly interacting Fermi gas we adiabatically ramp the magnetic field to the peak of the Feshbach resonance where the s-wave scattering length  $a$  diverges and the dimensionless interaction parameter  $1/k_F^0 a = 0$ . Here  $k_F^0$  is the Fermi wave vector that corresponds to the peak density of the original weakly interacting gas. Previous measurements have shown that after the ramp to  $1/k_F^0 a = 0$ , our Fermi gas will be at  $(0.9 \pm 0.1) \cdot T_c$  for the superfluid state [2]. With photoemission spec-

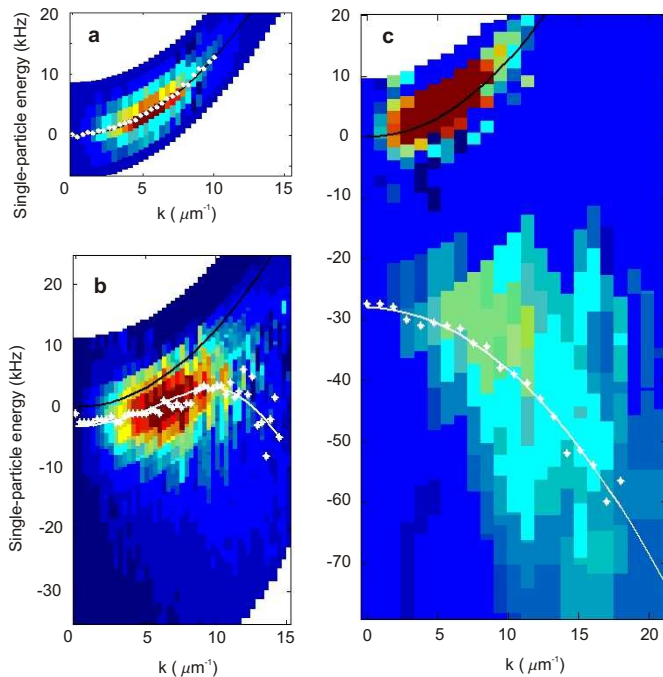


FIG. 3: **Single-particle excitation spectra obtained using photoemission spectroscopy for ultracold atoms.** Plotted are intensity maps (independently scaled for each plot) of the number of atoms out coupled to a weakly-interacting spin state as a function of the single-particle energy  $E_s$  and wave vector  $k$ . The black lines are the expected dispersion curve for an ideal Fermi gas. The white points (\*) mark the center of each fixed energy distribution curve. **a** Data for a very weakly-interacting Fermi gas. The Fermi wave vector  $k_F^0$  is  $8.6 \pm 0.3 \mu\text{m}^{-1}$ . **b** Data for a strongly interacting Fermi gas  $1/k_F^0 a = 0$  and  $T \approx T_c$ . The white line is a fit of the centers to a BCS-like dispersion. **c** Data for a gas on the BEC side of the resonance where  $1/k_F^0 a \approx 1$  and the measured two-body binding energy is  $h \cdot (25 \pm 2 \text{ kHz})$ . We attribute the upper feature to unpaired atoms and the lower feature to molecules. The white line is a fit to the centers using a quadratic dispersion.

troscopy on the strongly interacting gas we extract the intensity map shown in Fig. 3b. The interactions lower the overall energy and flatten the dispersion curve. In addition, the energy width is broadened well beyond our energy resolution.

There is now a wide consensus that interpretation of previous rf spectroscopy measurements [3, 16, 17] in terms of a pairing gap is a difficult problem that is still unsolved theoretically [27]. The photoemission spectroscopy technique presented here directly measures the occupied single-particle density of states and is therefore well-suited for measuring pairing gaps. In BCS theory the gap vanishes at  $T_c$ ; however, in the BCS-BEC crossover a pseudogap due to preformed pairs is predicted to exist above  $T_c$  [11, 28]. Perali *et al.* calculated the spectral function for a homogeneous Fermi gas near  $T_c$  and found that the peaks of the spectral function fit

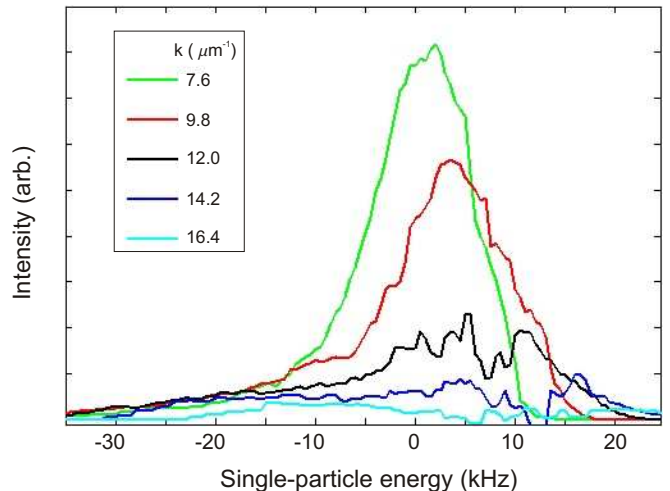


FIG. 4: **Energy distribution curves for a strongly interacting Fermi gas.** We plot the intensity for selected values of  $k$ . Each curve is the average for seven neighboring values of  $k$  in Fig. 3b. The data have been smoothed with a 1.5 kHz wide filter.

almost exactly to a “BCS-like” dispersion curve where the BCS gap was replaced by the pseudogap [11]. As a first step to analyzing our data, we fit the centers of the intensity at each value of  $k$  to this BCS-like dispersion curve [11],  $E_s = \mu' - \sqrt{(\epsilon_k - \mu')^2 + \Delta^2}$ . Here, the fitting parameters are the renormalized chemical potential  $\mu'$  and the pseudogap  $\Delta$ . The best fit, shown as the white curve in Fig. 3b, gives  $\mu' = h \cdot (12.6 \pm 0.7 \text{ kHz})$  and  $\Delta = h \cdot (9.5 \pm 0.6 \text{ kHz})$ . In Fig. 14 of Ref. [11], Perali *et al.* also plot an example of predicted spectral functions for a few values of wave vector  $k$ . To facilitate comparison with theory, in Fig. 4 we show measured energy distribution curves (EDCs) for select values of  $k$ . It should be noted that in all trapped gas experiments, the density is inhomogeneous and the pairing gap will depend on the local Fermi energy. Therefore, our data should eventually be compared with a theory that includes the effect of the trapping potential through, for example, a local density approximation. Finally, we note that we have performed photoemission spectroscopy for a gas cooled below  $T_c$  (initial  $T/T_F = 0.10$ ) and found that the data is qualitatively very similar to that in Fig. 3b.

Far on the BEC side of the resonance, for  $1/k_F^0 a \gg 1$ , the pairing gap eventually becomes a two-body binding rather than a many-body effect that depends on the local Fermi energy. We measure the excitation spectrum for the Fermi gas at  $1/k_F^0 a \approx 1$  where the molecule binding energy measured for a low density gas is  $h \cdot (25 \pm 2 \text{ kHz})$ . We observe two prominent features, see Fig. 3c. The first feature is narrow in energy, starts at zero energy, and follows the quadratic dispersion expected for free atoms (black line). We attribute this feature to unpaired atoms, which may be out of chemical equilibrium with the pairs. The second feature is very broad in energy, is shifted to

lower energy, and trends towards lower energy for increasing  $k$ . This feature we attribute to atoms in the paired state. An excitation gap separating the two features is evident in the data. We fit the centers of the molecule feature to a quadratic dispersion (white line) with the free parameters being the energy offset and an effective mass  $m^*$ . In the BEC limit, where one has tightly bound molecules, we would expect the energy offset to be the molecule binding energy, which equals  $2\Delta$ , and the effective mass to be  $-m$ . This negative effective mass reflects the fact that out coupling an atom at high  $k$  leaves behind an excitation in the form of an unpaired atom. The best fit to the data gives an energy offset of 28 kHz and  $m^* = -1.25 m$ .

The large energy width seen in Fig. 3c is likely due to center-of-mass motion of the pairs. For comparison with the data, we have performed a simple Monte Carlo simulation assuming a thermal distribution for the center-of-mass motion and using the predicted distribution of relative kinetic energy for rf dissociation of weakly bound molecules [20]. We assume the pairs are in thermal equilibrium with the unpaired atoms and use the measured temperature of the rf out-coupled atoms corresponding to the upper feature in Fig. 3c. Assuming a molecule binding energy of  $h \cdot (25 \text{ kHz})$ , the calculation gives the intensity map shown in Fig. 5a.

The occupied density of states is obtained by summing the data in Fig. 3 over all  $k$ , see Fig. 5b-d. For the nearly ideal Fermi gas data, Fig. 5b, we find good agreement with the expected density of states for a Fermi gas at  $T = 0.18 T_F$  in a harmonic trap (red curve). For the strongly interacting gas, Fig. 5c, the occupied density of states becomes wider in energy and the peak shifts towards lower energies by an amount comparable to  $E_F$ . From previous measurements of the in-trap size of the cloud [29] we estimate the Fermi energy of the strongly interacting gas to be  $h \cdot (12.4 \pm 0.7 \text{ kHz})$  (dashed line). For the BEC side of the resonance, Fig. 5d, a pairing gap between bound pairs and free atoms is readily apparent. The red curve is the expected density of states determined from the simulation of a thermal distribution of weakly bound molecules (Fig. 5a). The only free parameter in the simulation is an overall scaling factor.

In this work, we have used photoemission spectroscopy, accomplished by momentum resolving the out-coupled atoms in rf spectroscopy, to probe the occupied single-particle density of states and energy dispersion through the BCS-BEC crossover. In the future, it may be possible to use spatially resolved photoemission spectroscopy to probe the local pairing gap. Another extension of this work will be to study the BCS-BEC crossover as a function of temperature and/or unbalanced spin population. Photoemission spectroscopy for ultracold atoms is a powerful and conceptually simple probe of strongly correlated atom gases that could be applied to many other atom gas systems. In the studies presented here, the atoms are

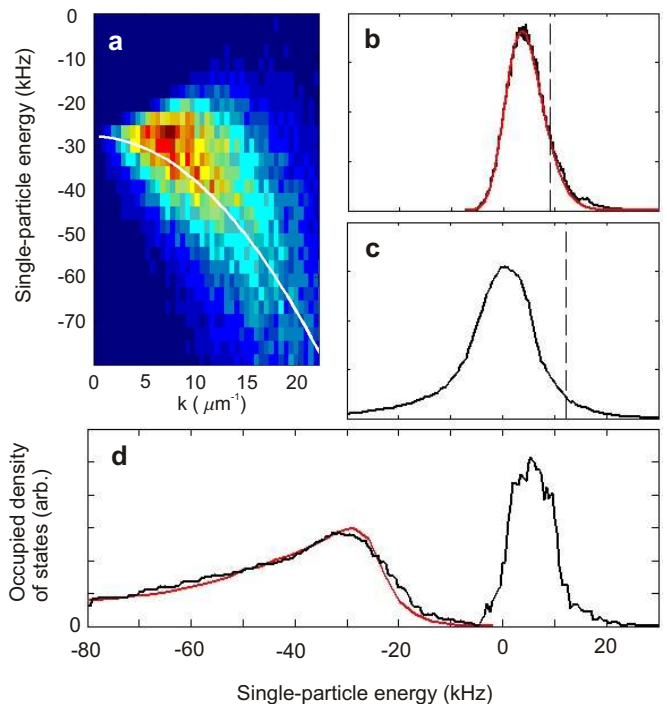


FIG. 5: **The occupied single-particle density of states.** **a** A calculated intensity map for a thermal distribution of weakly bound molecules is shown. The white line is the fit to the data shown in Fig. 3c. **b** The density of states for a weakly-interacting Fermi gas (black line) agrees well with a fit (red curve) for a Fermi gas in a harmonic trap. The fit, whose only free parameter is the amplitude, includes our measurement resolution. The dashed black vertical line shows  $E_F$ . **c** The density of states taken at the peak of the Feshbach resonance is shifted to much lower energy. **d** The density of states on the BEC side of the resonance has two features; a narrow peak due to unpaired atoms and a broader feature due to molecules. The red curve is the expected density of states from the simulation shown in **a**.

interacting via isotropic s-wave interactions and therefore considering different directions of the out-coupled atoms' momenta was not necessary. However, like angle-resolved photoemission spectroscopy (ARPES) for solids, this technique could also be applied to non-isotropic systems such as atoms in an optical lattice, low dimensional systems, or higher partial wave pairing of atoms [30].

## Methods

We evaporatively cool an equal mixture of  $^{40}\text{K}$  atoms in the  $|f, m_f\rangle = |9/2, -7/2\rangle$  and  $|f, m_f\rangle = |9/2, -9/2\rangle$  states, where  $f$  and  $m_f$  give the hyperfine level in the ground-state manifold. We cool the gas to in an optical dipole trap as described previously [29]. The frequencies for the cylindrically symmetric trap are  $f_r = 233 \text{ Hz}$  and  $f_z = 19 \text{ Hz}$ . The time-of-flight imaging uses a beam that propagates along the  $\hat{z}$  direction. At the end of

the evaporation, we adiabatically increase the interaction strength by lowering the magnetic field, at a rate of 0.1 G/ms, to a value near the Feshbach resonance located at  $202.10 \pm 0.07$  G [2]. The magnetic field values for the data in Fig. 3a-c are 208.43, 202.10, and 201.51 G, respectively.

For photoemission spectroscopy, we apply an rf pulse with a Gaussian amplitude envelope with a  $1/e^2$  width of 240  $\mu$ s, to transfer atoms from the  $|9/2, -7/2\rangle$  state to the  $|9/2, -5/2\rangle$  state. The rf frequency is approximately 47 MHz. Atoms in the  $|9/2, -5/2\rangle$  state have a two-body s-wave scattering length that is 130 Bohr radii with the  $|9/2, -7/2\rangle$  state and 250 Bohr radii with the  $|9/2, -9/2\rangle$  state. Immediately after the rf pulse we turn off the optical trap and let the atoms expand for 3 to 6.5 ms before taking a resonant absorption image of the  $|9/2, -5/2\rangle$  atoms. Typically four images are averaged for each rf frequency. For the weakly-interacting Fermi gas, the rf power was chosen to achieve maximum transfer. For data on resonance and on the BEC-side of resonance, no more than 30% of the atoms were transferred into the third spin state. At the higher rf frequencies, we increased the signal by increasing the rf power and then scaled the data to give the appropriate intensity.

In Eqn. 1, we take  $\phi$  to be the rf resonance energy measured for a weakly interacting gas. There is an uncertainty of  $\pm 1$  kHz in  $\phi$  and therefore also in the zero of  $E_s$ . The measured wave vector  $k$  has an uncertainty of approximately 5% from uncertainty in the magnification of the imaging system.

We acknowledge funding from the NSF. We thank Eric Cornell, Dan Dessau, and the JILA BEC group for discussions.

---

\* Electronic address: jin@jilau1.colorado.edu; URL: <http://jilawww.colorado.edu/~jin/>

- [1] C. A. Regal, C. Ticknor, J. L. Bohn, and D. S. Jin. Creation of ultracold molecules from a Fermi gas of atoms. *Nature* **424**, 47-50 (2003).
- [2] C. A. Regal, M. Greiner, and D. S. Jin. Observation of Resonance Condensation of Fermionic Atom Pairs. *Phys. Rev. Lett.* **92**, 040403 (2004).
- [3] C. Chin *et al.*. Observation of the Pairing Gap in a Strongly Interacting Fermi Gas. *Science* **305**, 1128-1130 (2004).
- [4] G. B. Partridge, K. E. Strecker, R. I. Kamar, M. W. Jack and R. G. Hulet. Molecular Probe of Pairing in the BEC-BCS Crossover. *Phys. Rev. Lett.* **95**, 020404 (2005).
- [5] M. W. Zwierlein, J. R. Abo-Shaer, A. Schirotzek, C. H. Schunck and W. Ketterle. Vortices and superfluidity in a strongly interacting Fermi gas. *Nature* **435**, 1047-1051 (2005).
- [6] L. Luo, B. Clancy, J. Joseph, J. Kinast, and J. E. Thomas. Measurement of the Entropy and Critical Temperature of a Strongly Interacting Fermi Gas. *Phys. Rev. Lett.* **98**, 080402 (2007).
- [7] L. Tarruell *et al.* Expansion of an ultra-cold lithium gas in the BEC-BCS crossover in *Proceedings of the International School of Physics "Enrico Fermi", Course CLXIV*, edited by W. K. M. Inguscio and C. Salomon (IOS Press, Amsterdam, 2008).
- [8] D. M. Eagles. Possible Pairing without Superconductivity at Low Carrier Concentrations in Bulk and Thin-Film Superconducting Semiconductors. *Phys. Rev.* **186**, 456-463 (1969).
- [9] A. J. Leggett. Cooper pairing in spin-polarized Fermi systems. *J. Phys. C (Paris)* **41**, C7-C19 (1980).
- [10] P. Nozieres and S. Schmitt-Rink. Bose condensation in an attractive fermion gas: from weak to strong coupling superconductivity. *J. of Low Temp. Phys.* **59**, 195211 (1985).
- [11] A. Perali, P. Pieri, G. C. Strinati, and C. Castellani. Pseudogap and spectral function from superconducting fluctuations to the bosonic limit. *Phys. Rev. B* **66**, 024510 (2002).
- [12] A. L. Fetter and J. D. Walecka, *Quantum Theory of Many-Particle Systems* (Dover Publications, Mineola, New York, 2003).
- [13] A. Damascelli. Probing the Electronic Structure of Complex Systems by ARPES. *Physica Scripta* **T109**, 61-74 (2004).
- [14] C. A. Regal and D. S. Jin. Measurement of Positive and Negative Scattering Lengths in a Fermi Gas of Atoms. *Phys. Rev. Lett.* **90**, 230404 (2003).
- [15] S. Gupta *et al.* Radio-Frequency Spectroscopy of Ultracold Fermions, *Science* **300**, 1723-1726 (2003).
- [16] Y. Shin, C. H. Schunck, A. Schirotzek W. and Ketterle. Tomographic rf spectroscopy of a trapped Fermi gas at unitarity. *Phys. Rev. Lett.* **99**, 090403 (2007).
- [17] C. H. Schunck, Y. Shin, A. Schirotzek, M. W. Zwierlein, and W. Ketterle. Pairing without superfluidity: The ground state of an imbalanced Fermi mixture. *Science* **316**, 867-870 (2007).
- [18] C. H. Schunck, Y. Shin, A. Schirotzek, and W. Ketterle. Determination of the fermion pair size in a resonantly interacting superfluid. arXiv:0802.0341v1.
- [19] T.-L. Dao, A. Georges, J. Dalibard, C. Salomon, and I. Carusotto. Measuring the One-Particle Excitations of Ultracold Fermionic Atoms by Stimulated Raman Spectroscopy. *Phys. Rev. Lett.* **98**, 240402 (2007).
- [20] C. Chin and P. S. Julienne. Radio-frequency transitions on weakly bound ultracold molecules. *Phys. Rev. A* **71**, 012713 (2005).
- [21] Z. Yu and G. Baym. Spin-correlation functions in ultracold paired atomic-fermion systems: Sum rules, self-consistent approximations, and mean fields. *Phys. Rev. A* **73**, 063601 (2006).
- [22] M. Punk and W. Zwerger. Theory of rf-spectroscopy of strongly interacting fermions. *Phys. Rev. Lett.* **99**, 170404 (2007).
- [23] A. Perali and G. C. Strinati. Competition between final-state and pairing gap effects in the radio-frequency spectra of ultracold Fermi atoms. *Phys. Rev. Lett.* **100**, 010402 (2008).
- [24] S. Basu and E. J. Mueller. Final-state effects in the radio frequency spectrum of strongly interacting fermions. arXiv: 0712.1007v1.
- [25] M. Veillette *et al.* Radio frequency spectroscopy of a strongly imbalanced Feshbach-resonant Fermi gas. arXiv:0803.2517v1.

- [26] Y. He, C.-C. Chien, Q. Chen, and K. Levin. Temperature and final state effects in radio frequency spectroscopy experiments on atomic Fermi gases. arXiv:0804.1429v1.
- [27] S. Giorgini, L. P. Pitaevskii, and S. Stringari. Theory of ultracold Fermi gases. *Rev. Mod. Phys.* in press (2008).
- [28] Q. Chen, J. Stajic, S. Tan, and K. Levin. BCS-BEC crossover: From high temperature superconductors to ultracold superfluids. *Phys. Rep.* **412**, 1-88 (2005).
- [29] J. T. Stewart, J. P. Gaebler, C. A. Regal, and D. S. Jin. Potential Energy of a  $^{40}\text{K}$  Fermi Gas in the BCS-BEC Crossover. *Phys. Rev. Lett.* **97**, 220406 (2006).
- [30] J. P. Gaebler, J. T. Stewart, J. L. Bohn, and D. S. Jin. p-wave Feshbach molecules. *Phys. Rev. Lett.* **98**, 200403 (2007).